VISCOSITY EFFECT ON DISPLACEMENTS AND STRESSES OF A TWO-PASS WELDING PLATE

Walid El Ahmar, Jean-François Jullien
LaMCoS, CNRS UMR 5514, INSA-Lyon
20 Avenue Albert Einstein, 69621 Villeurbanne Cedex, France,
Email: walid.el-ahmar@insa-lyon.fr, jean-francois.jullien@insa-lyon.fr

Keywords

Welding viscosity, Multipass welding, 3D welding simulation, stainless steel.

ABSTRACT

The highly localized transient heat and strongly nonlinear temperature fields in both heating and cooling processes cause nonuniform thermal expansion and contraction, and thus result in plastic deformation in the weld and surrounding areas. Consequently, residual stress, strain and distortion are permanently produced in the welded structures. High tensile residual stresses are known to promote fracture and fatigue, while compressive residual stresses may induce undesired, and often unpredictable, global or local buckling during or after the welding. It is particularly evident with large and thick panels, as used in the construction of nuclear building. These adversely affect the fabrication, assembly, and service life of the structures. Therefore, prediction and control of residual stresses and distortion from the welding process are extremely important for the nuclear installation's security.

This study focuses on the three-thermo-mechanical behavior of 316L stainless steel, during a TIG welding process. In this paper we investigate the effect of viscosity property on experimental and numerical results. Therefore, a parallel experimental and numerical study is carried out on an industrial 24-25 mock-up benchmark [1], a test more representative of a real welding operation, considering repair welding, is implemented to validate three-dimensional numerical effect. The TIG process, with 316L material filler, is considered. Comparative analyses through numerical simulations using finite element code (version 7.4 code_Aster from EDF) are performed.

Introduction

A two pass weld using the TIG process with 316L material filler is made along the groove (Figure. 2) of a low-carbon austenitic stainless steel (type 316LNSPH) plate in the longitudinal direction. We usually named this test as "24-25" mock-up. The weld begins on the appendix and ends 10mm from the plate edges. The welding parameters used for the trial are U = 9V, I = 155A, and a welding speed of 0,667mm.s^{-1}. The plate is lying on three points in its lower face as shown in Figure.1. Temperatures are continuously recorded during the welding, using thermocouples (kind K (±*15%*)) in same points of the plate surface (Figure.4a). It is shown show that transient temperatures for both passes are quite the same. The hypothesis of steady state can then be assumed for the thermal modeling.
Welding parameters (Tension, Intensity, traveling speed of the torch) are also continuously recorded during the test. After cooling of the second pass, the residual stresses in the middle section perpendicular to the welding direction of the plates are measured with X-rays (±*50MPa*).
The role of the thermocouple T4 and the captor D6 is to verify that the symmetry is conserved.
The chemical composition of this 316L SPH material is presented on the table 1:

Comp.	C	Si	Mn	P	S	Cr	Ni	Mo	N
316L SPH	**0.024**	**0.38**	**1.76**	**0.023**	**0.001**	**17.31**	**12.05**	**2.55**	**0.07**

Table 1: Chemical composition of the 316L material

Geometry and boundary conditions

The experiment specimen is a plate with dimensions: 270 x 200 x 30 mm. The figure 1 presents the geometry of the plate which supports with three points on its lower face. The figure2 presents the groove geometry.

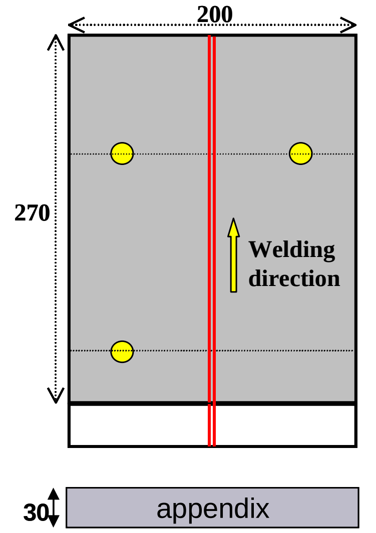

Figure 1 : Geometry of the plate (mm)

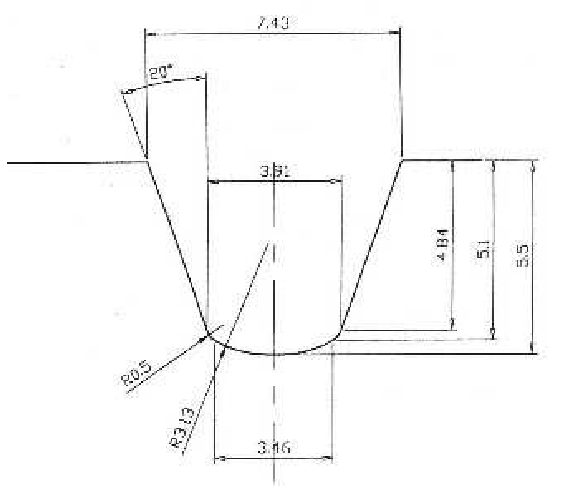

Figure 2: Groove geometry (mm).

Numerical simulations

An uncoupled thermo-mechanical analysis is considered in this study. The thermal analysis is performed at first, during which the time-dependent temperature field is saved for the subsequent mechanical analysis (stresses, displacements) [4].

Due to the symmetry of the plate, only one half was modeled. The mesh consists of quadratic prismatic elements, with 1800 HEXA20. 5 quadratic elements are set through the thickness. To perform the thermal analysis, we consider as the first stage of the numerical process a quasi-stationary problem, in order to adjust faster the parameters of the heat input. An arc efficiency term η is determined to take into account the losses. Afterwards, the non-stationary thermal process is considered from the beginning of the heating to the end of the cooling. The transient time-dependent temperature field is then saved for the subsequent complete three-dimensional thermo-mechanical analysis.

Modeling of the heat input

For the modeling of the heat source, it is of course possible to consider different kinds of mathematical models, from surface, like a Gaussian heat source, to volumetric, like the double ellipsoid from Goldak. Different kinds of modeling of the heat source have been considered for the thermal steady state calculation, with an efficiency parameter η fitted so as to adjust the simulated temperatures considering the measured ones, on some points of the surface plate (figure.4a). It appeared that the way the heat flux density was spread (in surface or in volume) had little effect on the macroscopic simulated temperature field, if the net total heat flux ηUI was the same. For that raison, the chosen heat source modeling for the 3-Dimensionnal transient thermal calculation was rather simple: we choosed a voluminal heat flux density, with a triangular aspect (Figure.3). Furthermore, the rather small penetration of the weld pool can justify a surface heat flux density. We suppose no heat exchange on the plane of symmetry (adiabatic thermal boundary conditions), and thermal transfer by radiation and convection for other faces, with an emissivity ε = 0,7 and a convective coefficient h = 15W.°C^{-1}.m^{-2}.

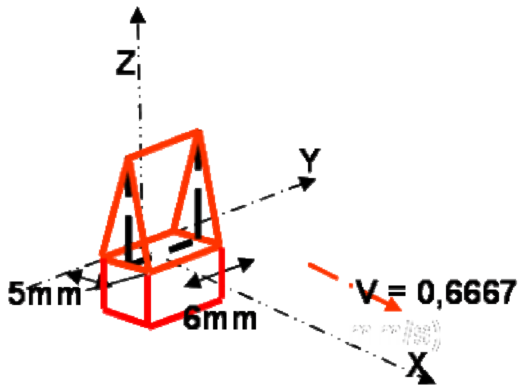

Figure.3: Heat source modeling for “24-25” mock-up

Thermal adjustment

Figures.4b & 4c compares the evolution of measured and calculated temperatures, for the transient analyses. The temperatures measured in the lower face were used to fit the heat input modeling, and that’s why there is a very good agreement with the experimental results. In the upper face, there is also a good agreement between simulation and measurements. No temperature measurement was possible closer to the fusion line.

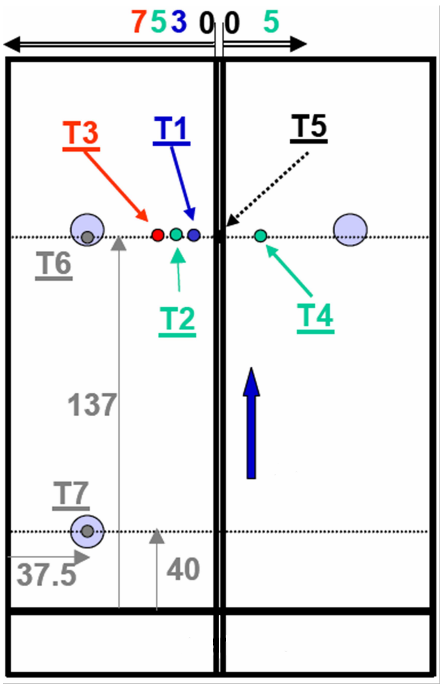

Figure. 4a: Thermal instrumentation (mm)

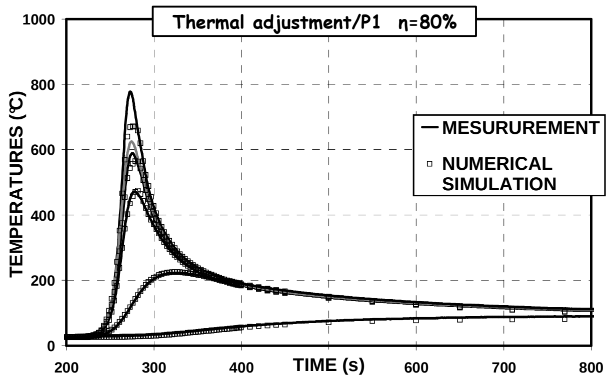

Figure. 4b : 1st pass

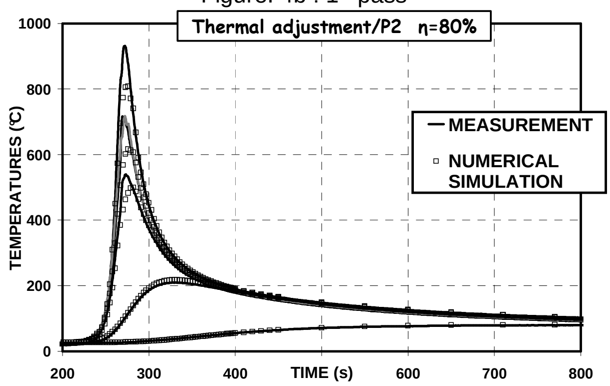

Figure. 4c : 2nd pass

Mechanical analysis

Different modeling kinds of 24-25 mock-up are considered in this study. A complete three-dimensional simulation is performed; firstly without considered time-dependant plasticity, kinematics (C) or isotropic (I) hardening. Secondly taking into account, a time-dependant plasticity for high temperatures, by the use of an elasto-viscoplastic with Norton viscosity (V-C, V-I).
For the second pass and after cooling, all the numerical results are compared to experimental results given by a similar mock-up.

Mechanical proprieties

All requisite material characteristic data including their temperature dependency have been deduced form characterization of the 316L steel in our laboratory [2]. Dilatation tests provided expansion coefficient, and traction tests(Figure.5) at various temperatures have been realized in order to obtain elasto-plastic data from 20℃ to 1000℃, that is: Y oung's modulus, yield stress, linear hardening's modulus. Viscoplastic data have been deduced from creeping and relaxing tests above 500℃, as viscosity effect was not taken into account below this temperature ($\nu = 0$ for T<500℃). The yield of vicoplastic flow is set to zero for T > 1000℃, the behavior is then purely vi scoplastic above this temperature.

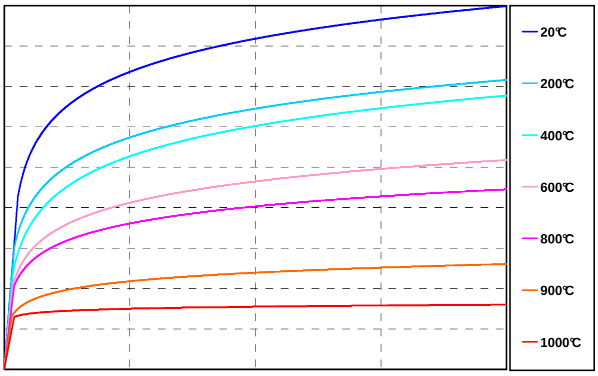

Figure.5: Tensile behaviors of 316L "INSA", private database (BIFE) [2]

In this study, we simplify the real mechanical behavior on a bilinear mechanical behavior law as shown in Figure 6.

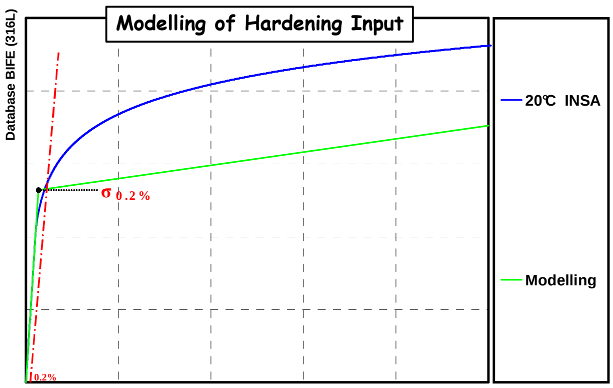

Figure.6: Modeling of hardening input

Displacements

Captor D3 (Figure.5a) provides the displacement under the fusion line, on the centre. The calculated transient vertical displacement on D3 position, relative to the two passes[5], compared to the measured ones, as shown in Figures 7b and 7c, is satisfactory agreement. In particular, considering **viscosity** in the material behavior reduce error between calculation and experiment.
The three-dimensional effects, which result in flexion effects, are well reproduced.

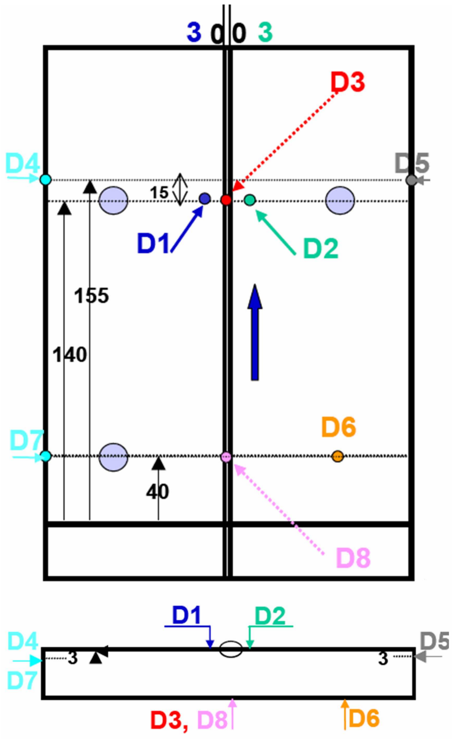

Figure. 7a: Displacement instrumentation (mm)

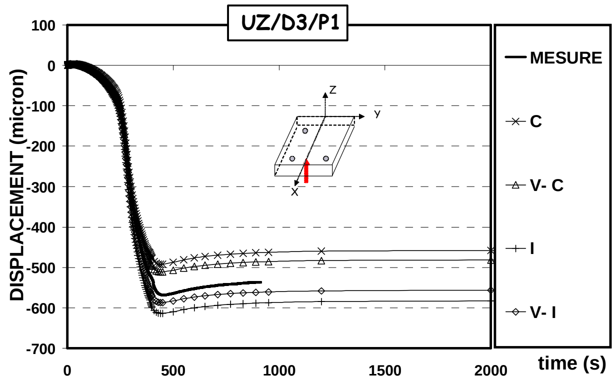

Figure. 7 b : 1st pass

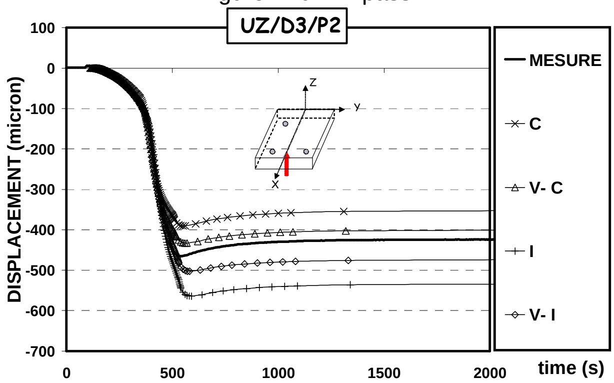

Figure. 7c : 2nd pass

Stress

The shape and level of calculated residual stresses in a horizontal median face (Figure. 8), shows that the stress state is mainly longitudinal. The repartition of longitudinal stresses is close to the repartition of tangential residual stresses. The level of transverse residual stresses is lower, and other components of the residual stress tensor are negligible. The stress gradient through the thickness is low. Flexion effects in the longitudinal direction seem to have a non-negligible influence on the final stress state.

To validate the numerical simulation we need same experimental measurements for comparing. The Figure.8 shows us that SIXX and SIYY are the tow important components of the stress tensor. So after cooling of the second pass only, the SIXX and SIYY residual stresses in the perpendicular middle section to the welding direction of the plate are measured with X-rays diffraction technique (±*50MPa*).

In this paper we will particularly focus our study in the most important component of the stress tensor; the longitudinal residual stress: SIXX.

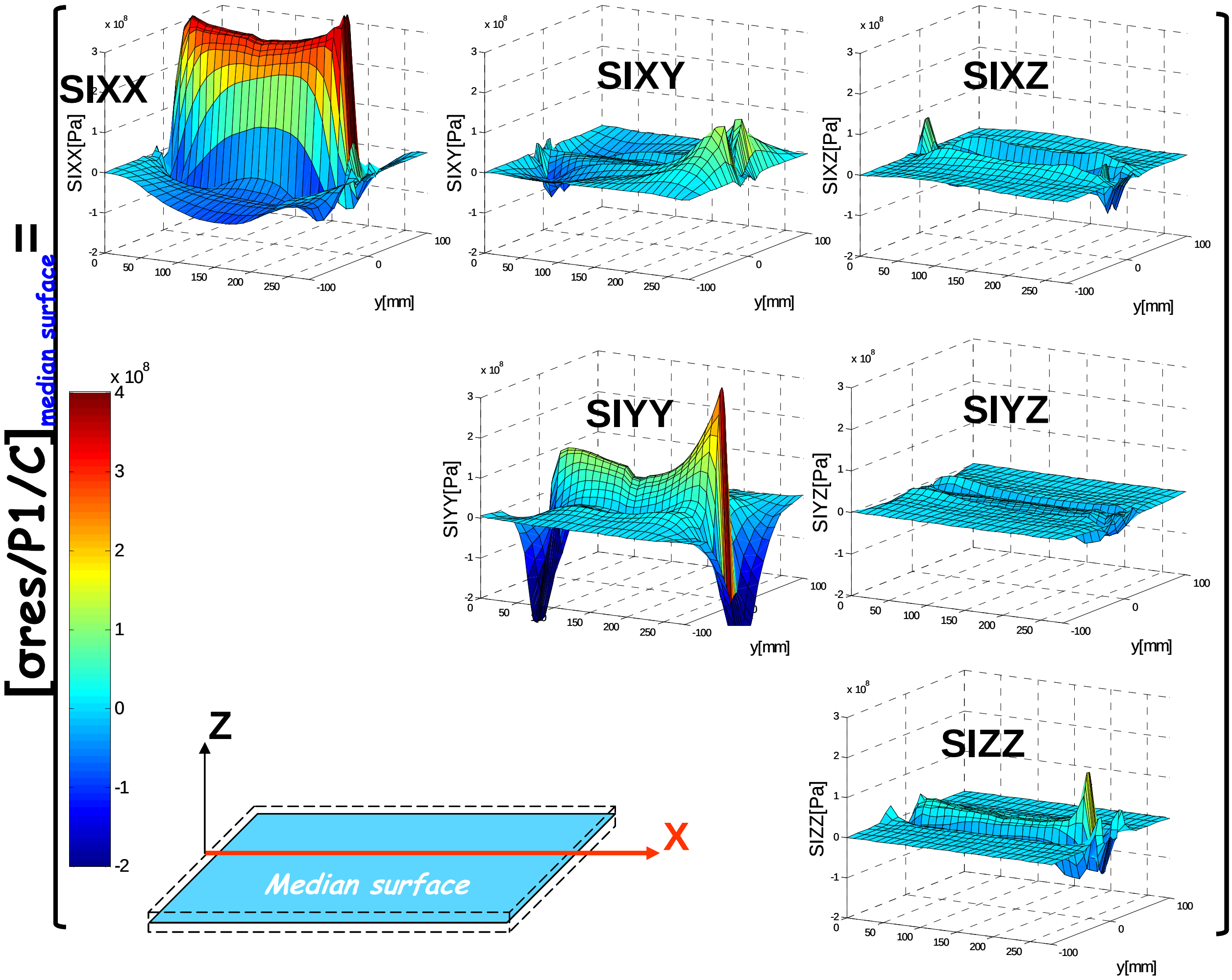

Figure.8: Residual stress tensor

Experimental results

Figures.9a and 9b represent respectively the longitudinal residual stresses (in the direction of the weld), and the transverse residual stresses (orthogonal to the welding direction, in the lower face of a cross section). The measured residual stress field (relative to another similar mock-up with 4 passes) is mainly longitudinal, in the welding direction, with a typical pattern of tensile stresses near the weld and compressive stresses in the edges. Longitudinal stresses are tensile stresses at the weld centerline, and drop to compressive values about 30 mm from the centerline, reaching approximately –200MPa. The tensile transverse stresses are much lower, even in the center.

It is for common use to neglect viscous effects when simulations of welding are performed, mainly because viscous parameters are difficult to obtain [6], [7]. For this reason we make two same tests but with different speeds to test the effect of viscosity on the residual state of stress as shown in Figure.9.
We conclude that the viscosity (synonym at the speed of torch) has a neglect effect on the longitudinal and transversal residual stresses.

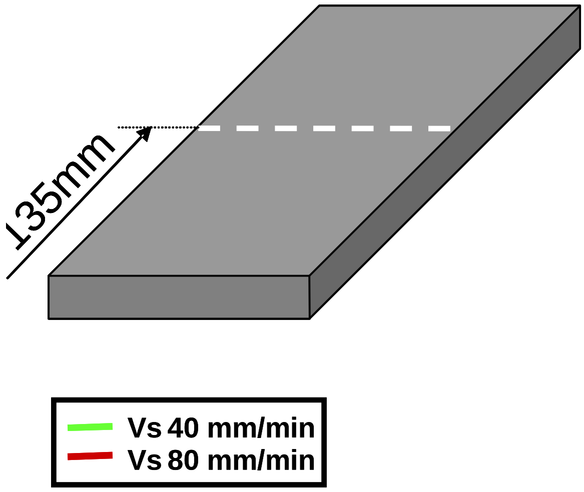

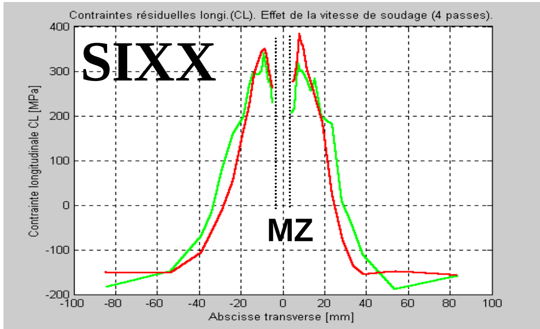

Figure. 9b : Longitudinal stress

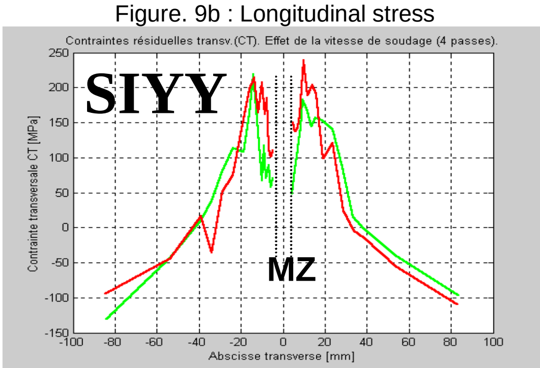

Figure. 9a: Position of X-rays measurement

Figure. 9c : Transversal stress

Figure.9: Effect of torch speed on the measurement of residual stress (SIXX, SIYY)

Numerical analyses

Figure10b compares the longitudinal residual stress given by different kinds of modeling to the experimental results. We conclude that the viscous data have a localized effect in the HAZ zone, which is a very good agreement with the experimental results (Figure.9).

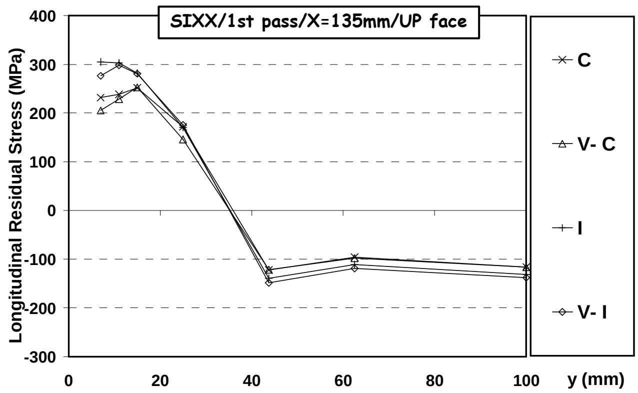

Figure. 10a: 1^{st} pass

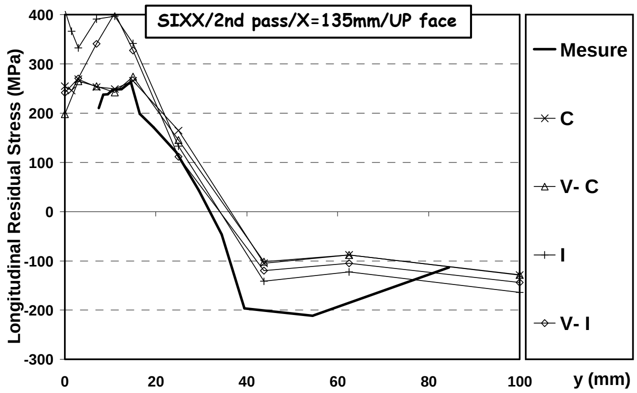

Figure. 10b: 2^{nd} pass

Figure.10: Effect of modeling kinds on the residual stress SIXX

If viscous data are not available, it seems better to use kinematic hardening (C) for calculating residual stresses during simulating multipasse welding, as isotropic hardening would lead to an increasing of the residual stress after each cycle.

Therefore elastoplastic with kinematic hardening (C), can then be used with quite enough confidence to simulate welding.

Conclusions

In the thermal analysis, different kinds of modeling of the heat source have been considered for the thermal steady state calculation, with an efficiency parameter η fitted so as to adjust the simulated temperatures considering the measured ones. It appeared that the way of the spread heat flux density had little effect on the macroscopic simulated temperature field, if the net total heat flux ηUI was the same.

In the mechanical analysis, 24-25 mock-up allow us to test the effect of viscosity on displacements and stress results, the different conclusions are:

- Considering viscosity in the material behavior reduce error between calculation and experiment displacements.
- The stress state is mainly longitudinal.
- Measurement analyses show us that the viscosity (synonym of the torch speed) has a neglect effect on the longitudinal and transversal residual stresses.
- Numerical analyses show us that the viscosity have a localized effect in the HAZ zone.
- Elastoplastic modeling with kinematic hardening (C), can be used with quite confidence to simulate welding.

Acknowledgments

We thank EADS/CCR, EDF/SEPTEN, ESI-Group, FRAMATOME-ANP for their funding of this research effort and CEA, EDF/R&D for their experimental support.

References

1. Ayrault D., Blanchot O., Maquettes instrumentées de soudage multi-passe. Base de données expérimentale destinée à la validation de calculs.Projet : intégrité mécanique des tuyauteries fiche-action : CEA/EDF 2425, DECS/UTA /02-RT – 07.
2. El-ahmar, W., Base de données 316L, Comportement des matériaux situés dans la zone affectée thermiquement lors d'une opération de soudage, Note INSA Lyon, N°: I NSAVALOR257.8A401
3. Y.Vincent, J-F.Jullien, P.Gilles, "Thermo-mechanical consequences of phase transformations in heat-affected zone using a cyclic uniaxial test," International Journal of Solids and Structures*,* 42 (2005) 4077-4098.
4. L.Depradeux, J-F.Jullien, "Experimental and numerical simulation of thermomechanical phenomena during a TIG welding process,*"* J.Phys.IV France 120 (2004) 697-704
5. X.Desroches, "Note méthodologique sur la simulation numérique du soudage multipasses, " HI-75/01/017/A, EDF R&D.
6. L.E.Lindgren, "Finite element modelling and simulation of welding, Part 1: increased complexity," Journal of thermal stresses, 24, 2001, p.141-192.
7. L.E.Lindgren, "Finite element modelling and simulation of welding, Part 2: improved material modelling," Journal of thermal stresses, 24, 2001, p.195-131.